Perfectly Matched Layers for $\mathbf{T}, \Phi$ Formulation

Gernot Matzenauer, Oszkár Bíró, Karl Hollaus, Kurt Preis and Werner Renhart
Institute for Fundamentals and Theory in Electrical Engineering, Kopernikusgasse 24/3, A-8010 Graz, Austria
E-mail: matzenauer@TUGraz.at

***Abstract*: Perfectly Matched Layers (PMLs) are used for reflectionless truncation of the problem boundaries in FEM applications. The basic concept behind PMLs is to create an artificial material with a complex and diagonal anisotropic permittivity and permeability. For the $\mathbf{A}, V$ formulation PMLs are well known. In this paper the method of perfectly matched layers is extended to truncate any lossless medium and the method is implemented for the $\mathbf{T}, \Phi$ formulation.**

***Keywords*: Perfectly Matched Layer, Finite Element Method, $\mathbf{T}, \Phi$ formulation, Perfectly Matched Anisotropic Absorber, Absorbing Boundary Condition**

I. Introduction

In the present paper, an artificial anisotropic lossy material has been applied to a 3D edge finite-element $\mathbf{T}, \Phi$ formulation [1] to form perfectly matched layers. This material fully absorbs the electromagnetic field impinging on it without reflections on the PML-air interface [2].

The permittivity $[\underline{\boldsymbol{\epsilon}}]$ and the permeability $[\underline{\boldsymbol{\mu}}]$ in PMLs are considered as complex diagonal tensors. The following condition is required to match the intrinsic impedances of vacuum and the PML[2]:

$$\frac{\mu_0}{\epsilon_0}[\mathbf{1}] = [\underline{\boldsymbol{\mu}}][\underline{\boldsymbol{\epsilon}}]^{-1} \tag{1}$$

where $[\mathbf{1}]$ is the unit tensor. Thus, the permittivity $[\underline{\boldsymbol{\epsilon}}]$ and the permeability $[\underline{\boldsymbol{\mu}}]$ can be written as

$$[\underline{\boldsymbol{\epsilon}}] = \epsilon_0 \begin{bmatrix} a & 0 & 0 \\ 0 & b & 0 \\ 0 & 0 & c \end{bmatrix} = \epsilon_0[\mathbf{\Lambda}],$$

$$[\underline{\boldsymbol{\mu}}] = \mu_0 \begin{bmatrix} a & 0 & 0 \\ 0 & b & 0 \\ 0 & 0 & c \end{bmatrix} = \mu_0[\mathbf{\Lambda}]. \tag{2}$$

Here a, b and c are complex numbers describing the material properties of the anisotropic absorber. Consequently, Maxwell's equations in the PML are

$$\begin{aligned} \nabla \times \mathbf{H} &= j\omega\epsilon_0[\mathbf{\Lambda}]\mathbf{E} \\ \nabla \times \mathbf{E} &= -j\omega\mu_0[\mathbf{\Lambda}]\mathbf{H} \\ \nabla \cdot \epsilon_0[\mathbf{\Lambda}]\mathbf{E} &= 0 \\ \nabla \cdot \mu_0[\mathbf{\Lambda}]\mathbf{H} &= 0. \end{aligned} \tag{3}$$

The Maxwell equations are not modified with this approach and the implementation is straightforward in existing solvers with finite element methods (FEM). It is sufficient for the code to permit complex anisotropic materials. In this paper the method of perfectly matched layers is extended to truncate any lossless medium and the method is implemented for the $\mathbf{T}, \Phi$ formulation. The results are illustrated by two numerical examples.

II. Proof of the perfect matching property

Based on [2] it is shown below that the PML interface also works with any lossless material in front of the PML. Similarly to (2), the permittivity and permeability tensors of the PML are assumed to be:

$$\begin{aligned} [\underline{\boldsymbol{\epsilon}}] &= \epsilon_0\epsilon_r[\mathbf{\Lambda}], \\ [\underline{\boldsymbol{\mu}}] &= \mu_0\mu_r[\mathbf{\Lambda}]. \end{aligned} \tag{4}$$

The question is how to choose the parameters a, b, c, μ_r and ϵ_r, so that no reflection occurs on an interface between the PML and a medium with permeability μ_r^* and permittivity ϵ_r^*. The wave equations for the electric and the magnetic field in the PML are:

$$\begin{aligned} [\mathbf{\Lambda}]^{-1}\nabla \times [\mathbf{\Lambda}]^{-1}\nabla \times \mathbf{E} - \omega^2\mu_0\,\mu_r\epsilon_0\,\epsilon_r\mathbf{E} &= \mathbf{0}, \\ [\mathbf{\Lambda}]^{-1}\nabla \times [\mathbf{\Lambda}]^{-1}\nabla \times \mathbf{H} - \omega^2\mu_0\,\mu_r\epsilon_0\,\epsilon_r\mathbf{H} &= \mathbf{0}. \end{aligned} \tag{5}$$

General solutions for the electric and the magnetic field can be constructed from plane waves of the form

$$\begin{aligned} \mathbf{E} &= \mathbf{E}_0\, e^{j(\omega t - \mathbf{kr})} \\ \mathbf{H} &= \mathbf{H}_0\, e^{j(\omega t - \mathbf{kr})} \end{aligned} \tag{6}$$

where $\mathbf{k} = k_x\,\mathbf{e_x} + k_y\,\mathbf{e_y} + k_z\,\mathbf{e_z}$, $\mathbf{r} = x\,\mathbf{e_x} + y\,\mathbf{e_y} + z\,\mathbf{e_z}$ and $\mathbf{E}_0$ and $\mathbf{H}_0$ are constant vectors. The dispersion relation of the PML leads to an equation of the form:

$$\frac{k_x^2}{bc} + \frac{k_y^2}{ac} + \frac{k_z^2}{ab} = k_0^2. \tag{7}$$

where

$$k_0^2 = \omega^2\mu_0\,\mu_r\,\epsilon_0\,\epsilon_r \tag{8}$$

is the propagation constant. The solution of the dispersion relation is:

$$\begin{aligned} k_x &= k_0\sqrt{bc}\sin\theta\cos\phi \\ k_y &= k_0\sqrt{ac}\sin\theta\sin\phi \\ k_z &= k_0\sqrt{ab}\cos\theta \end{aligned} \tag{9}$$

To find out which component of the electric field belongs to which component of the magnetic field, the solutions for the electric and the magnetic field (6) are inserted into Maxwell's equations. Using Faraday's law yields

$$H_x = \frac{1}{Z_0}\left(E_z\sqrt{\frac{c}{a}}\sin\theta\sin\phi - E_y\sqrt{\frac{b}{a}}\cos\theta\right), \tag{10}$$

$$H_y = \frac{1}{Z_0}\left(E_x\sqrt{\frac{a}{b}}\cos\theta - E_z\sqrt{\frac{c}{b}}\sin\theta\cos\phi\right),$$

$$H_z = \frac{1}{Z_0}\left(E_y\sqrt{\frac{b}{c}}\sin\theta\cos\phi - E_x\sqrt{\frac{a}{c}}\sin\theta\sin\phi\right).$$

Using Ampere's law leads to

$$E_x = Z_0 \left(H_y \sqrt{\frac{b}{a}} \cos\theta - H_z \sqrt{\frac{c}{a}} \sin\theta \sin\phi \right), \quad (11)$$

$$E_y = Z_0 \left(H_z \sqrt{\frac{c}{b}} \sin\theta \cos\phi - H_x \sqrt{\frac{a}{b}} \cos\theta \right),$$

$$E_z = Z_0 \left(H_x \sqrt{\frac{a}{c}} \sin\theta \sin\phi - H_y \sqrt{\frac{b}{c}} \sin\theta \cos\phi \right).$$

where

$$Z_0 = \sqrt{\frac{\mu_0 \, \mu_r}{\epsilon_0 \, \epsilon_r}} \quad (12)$$

is the wave impedance of the PML.

Let us consider a plane wave incident on a PML as shown in Fig. 1. The values of a, b, c, μ_r and ϵ_r are to be determined so that independent of the incident angle α_e no reflection occurs on the interface. The reflection coefficient r and the transmission coefficient t are defined by:

$$r = \frac{E_{0r}}{E_{0e}}$$
$$t = \frac{E_{0t}}{E_{0e}} \quad (13)$$

where E_{0e}, E_{0r} and E_{0t} are the magnitudes of the exciting, the reflected and the transmitted electric field. The condition for no reflection is that the reflection coefficient vanishes $r = 0$ and the transmission coefficient is $t = 1$. The propagation vectors are restricted to the $x - z$-plane. For the TE mode, the excited and the reflected waves are given by:

$$\mathbf{E}_{ey} = E_{0e} \, e^{-j \, \mathbf{k}\cdot\mathbf{r_e}} \quad (14)$$

$$\mathbf{H}_{ex} = -\frac{1}{Z_0^*} E_{0e} \, \cos\alpha_e \, e^{-j \, \mathbf{k}\cdot\mathbf{r_e}}$$

$$\mathbf{H}_{ez} = \frac{1}{Z_0^*} E_{0e} \, \sin\alpha_e \, e^{-j \, \mathbf{k}\cdot\mathbf{r_e}}$$

$$\mathbf{k}\cdot\mathbf{r_e} = k_0 (x \sin\alpha_e + z \cos\alpha_e)$$

$$\mathbf{E}_{ry} = E_{0r} \, e^{-j \, \mathbf{k}\cdot\mathbf{r_r}}$$

$$\mathbf{H}_{rx} = \frac{1}{Z_0^*} E_{0r} \, \cos\alpha_r \, e^{-j \, \mathbf{k}\cdot\mathbf{r_r}}$$

$$\mathbf{H}_{rz} = \frac{1}{Z_0^*} E_{0r} \, \sin\alpha_r \, e^{-j \, \mathbf{k}\cdot\mathbf{r_r}}$$

$$\mathbf{k}\cdot\mathbf{r_r} = k_0^* (x \sin\alpha_r - z \cos\alpha_r)$$

where

$$k_0^{*^2} = \omega^2 \mu_0 \, \mu_r^* \, \epsilon_0 \, \epsilon_r^* \quad (15)$$

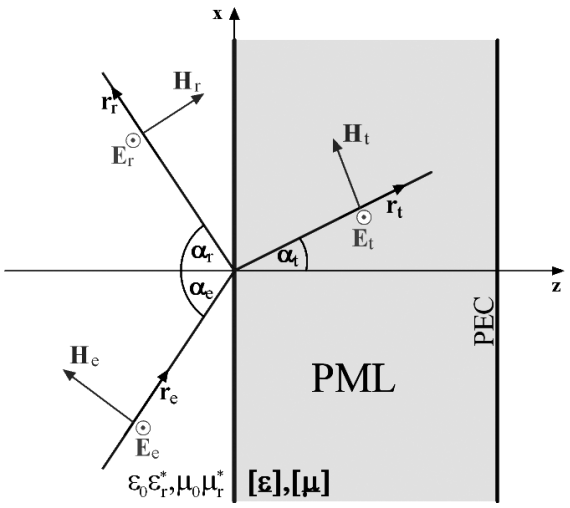

Figure 1. Plane wave in TE mode incidence on a z-plane interface.

is the propagation vector and $\mathbf{r_e}$ and $\mathbf{r_r}$ are the directions of the exciting and the reflected wave. The transmitted wave is given by:

$$\mathbf{E}_{ty} = E_{0t} \, e^{-j \, \mathbf{k}\cdot\mathbf{r_t}} \quad (16)$$

$$\mathbf{H}_{tx} = -\frac{1}{Z_0} E_{0t} \sqrt{\frac{b}{a}} \cos\alpha_t \, e^{-j \, \mathbf{k}\cdot\mathbf{r_t}}$$

$$\mathbf{H}_{tz} = \frac{1}{Z_0} E_{0t} \sqrt{\frac{b}{c}} \sin\alpha_t \, e^{-j \, \mathbf{k}\cdot\mathbf{r_t}}$$

$$\mathbf{k}\cdot\mathbf{r_t} = k_0 (x\sqrt{bc} \sin\alpha_t + z\sqrt{ab} \cos\alpha_t)$$

where $\mathbf{r_t}$ is the direction of the transmitted wave. Here Z_0^* is the wave impedance of the lossless linear space:

$$Z_0^* = \sqrt{\frac{\mu_0 \, \mu_r^*}{\epsilon_0 \, \epsilon_r^*}}. \quad (17)$$

Enforcing the tangential continuity of $\mathbf{E}$ on the interface at the position $z = 0$ yields the relation:

$$e^{-jk_0^* \, x \sin\alpha_e} + r \, e^{-jk_0^* \, x \sin\alpha_r} = t \, e^{-jk_0 \, x\sqrt{bc} \sin\alpha_t}. \quad (18)$$

The phase matching condition of the tangential component of the electric field is given by:

$$k_0^* \, \sin\alpha_e = k_0^* \, \sin\alpha_r = k_0 \, \sqrt{bc} \, \sin\alpha_t. \quad (19)$$

Provided

$$\sqrt{bc} = 1 \quad (20)$$

and

$$\mu_r^* \, \epsilon_r^* = \mu_r \, \epsilon_r, \quad (21)$$

$$\alpha_e = \alpha_r = \alpha_t \quad (22)$$

is obtained, i.e. no reflection occurs. Using (19), (18) becomes

$$1 + r = t. \quad (23)$$

Enforcing the tangential continuity of $\mathbf{H}$ and using (19) leads to

$$\cos\alpha_e(1-r) = \frac{Z_0^*}{Z_0}\sqrt{\frac{b}{a}}\,t\cos\alpha_t. \quad (24)$$

The magnitude matching equations yield the reflection coefficient

$$r_{TE} = \frac{\cos\alpha_e - \frac{Z_0^*}{Z_0}\sqrt{\frac{b}{a}}\cos\alpha_t}{\cos\alpha_e + \frac{Z_0^*}{Z_0}\sqrt{\frac{b}{a}}\cos\alpha_t}. \quad (25)$$

For the TM mode the same procedure can be followed to determine the reflection coefficient:

$$r_{TM} = \frac{\frac{Z_0^*}{Z_0}\sqrt{\frac{b}{a}}\cos\alpha_t - \cos\alpha_e}{\frac{Z_0^*}{Z_0}\sqrt{\frac{b}{a}}\cos\alpha_t + \cos\alpha_e} \quad (26)$$

Using the requirement (22) the reflection coefficient is independent of the angle. By setting

$$a = b \quad (27)$$

and

$$Z_0 = Z_0^* \quad (28)$$

the interface will be perfectly reflectionless for any frequency and angle of incidence.

In summary, (20) and (27) lead to

$$a = b = \frac{1}{c} \quad (29)$$

and the relations (21) and (28) yield

$$\epsilon_r = \epsilon_r^*, \qquad \mu_r = \mu_r^*. \quad (30)$$

Any arbitrarily polarized plane wave can be decomposed into a linear combination of TE and TM modes. So under the conditions (29) and (30) the PML will work with any polarization.

The complex PML constants a, b and c with $a = e(1-j)$ are suggested to be selected in [3] to satisfy:

$$\frac{-\ln\rho_{ref}}{\left(\frac{1}{r_{max}}+\beta_{min}\right)2nh} \le e \le \frac{-\ln d}{\left(\frac{1}{r_{min}}+\beta_{max}\right)2h} \quad (31)$$

Therein, n is the number of PML layers, h is the thickness of one layer, ρ_{ref} is the maximal reflection coefficient, d is the maximal decay characterizing the element, r_{max} and r_{min} are the largest and the smallest distance to the excitation and β_{max} and β_{min} are propagation constants for the largest and the smallest frequency used.

III. METHOD

The approach based on using anisotropic material properties to describe the absorbing layer has been implemented in a joint vector and scalar formulation $\mathbf{T}, \Phi$ ($\mathbf{T}$: current vector potential, Φ: magnetic scalar potential) realized by edge and nodal finite elements [1]. Furthermore, the properties of the PML layer have been extended to truncate any lossless linear material.

The field quantities for the $\mathbf{T}, \Phi$ formulation are derived from the potentials as

$$\mathbf{H} = \mathbf{T} - grad\Phi, \qquad \mathbf{J} = curl\mathbf{T} \quad (32)$$

and satisfy the constitutive relations: $\mathbf{B} = [\underline{\boldsymbol{\mu}}]\mathbf{H}$, $\mathbf{D} = [\underline{\boldsymbol{\epsilon}}]\mathbf{E}$ and $\mathbf{E} = [\underline{\boldsymbol{\rho}}]\mathbf{J}$ where $[\underline{\boldsymbol{\mu}}]$,$[\underline{\boldsymbol{\epsilon}}]$ and $[\underline{\boldsymbol{\rho}}]$ are the tensors of permeability, permittivity and resistivity. The permeability and conductivity may be written in complex form:

$$[\underline{\boldsymbol{\sigma}}] = [\boldsymbol{\sigma_E}] + j\omega[\boldsymbol{\epsilon}], \qquad [\underline{\boldsymbol{\mu}}] = \frac{[\boldsymbol{\sigma_M}]}{j\omega} + [\boldsymbol{\mu}]. \quad (33)$$

A magnetic conductivity tensor $[\boldsymbol{\sigma_M}]$ is introduced to describe the material properties of the PML. The complex material tensor for the electric resistivity can be obtained from

$$[\underline{\boldsymbol{\rho}}] = \left([\underline{\boldsymbol{\sigma}}]\right)^{-1}. \quad (34)$$

The tensors of permeability and resistivity have to be complex in the whole region to imply wave propagation with the $\mathbf{T}, \Phi$ formulation.

The governing differential equations for the $\mathbf{T}, \Phi$ formulation are obtained from Faraday's law and from the vanishing divergence of the magnetic induction:

$$\nabla\times\left([\underline{\boldsymbol{\rho}}]\,\nabla\times\mathbf{T}\right) + j\,\omega\left([\underline{\boldsymbol{\mu}}]\mathbf{T}\right) - j\,\omega\left([\underline{\boldsymbol{\mu}}]\nabla\Phi\right) = \mathbf{0},$$
$$\nabla\cdot\left([\underline{\boldsymbol{\mu}}]\mathbf{T} - [\underline{\boldsymbol{\mu}}]\nabla\Phi\right) = 0. \quad (35)$$

The material properties of a perfectly matched layer can be obtained from the complex PML tensor $[\boldsymbol{\Lambda}]$:

$$[\boldsymbol{\Lambda}] = \begin{bmatrix} e(1-j) & 0 & 0 \\ 0 & e(1-j) & 0 \\ 0 & 0 & \frac{(1+j)}{2\,e} \end{bmatrix}. \quad (36)$$

The conductivity, the permeability and the permittivity in the anisotropic absorber are:

$$[\boldsymbol{\sigma_E}] = -\mathrm{Im}\left\{[\boldsymbol{\Lambda}]\right\}\,\epsilon_0\,\epsilon_r^*\,\omega$$
$$[\boldsymbol{\epsilon}] = \mathrm{Re}\left\{[\boldsymbol{\Lambda}]\right\}\,\epsilon_0\,\epsilon_r^*$$
$$[\boldsymbol{\sigma_M}] = -\mathrm{Im}\left\{[\boldsymbol{\Lambda}]\right\}\,\mu_0\,\mu_r^*\,\omega$$
$$[\boldsymbol{\mu}] = \mathrm{Re}\left\{[\boldsymbol{\Lambda}]\right\}\,\mu_0\,\mu_r^* \quad (37)$$

The electric and magnetic conductivity are negative in the direction of propagation, which implies the existence of dependent sources within the anisotropic absorber.

To evaluate the accuracy of the suggested method, results have been compared with the solution obtained by a 3D finite-element $\mathbf{A}, V$ formulation.

IV. Numerical Examples

A. Magic - T

To evaluate the accuracy of the PML, a waveguide hybrid junction known as Magic-T [4] has been investigated (see Fig. 2). The frequency range of the waveguide has been set to the X-Band ranging from $8.2\ GHz$ to $12.4\ GHz$. The dimensions of the waveguide are: $a = 22.86mm$, $b = 10.16mm$.

When a TE_{10} mode is incident in port 1 the electric field cannot excite the TE_{10} mode in port 4. Thus there is no coupling between these two ports. Similarly to port 4, port 2 and port 3 are truncated with PMLs. If the PMLs do not work properly, there are reflections on port 2 and port 3. These reflected waves can excite the TE_{10} mode in arm 4 and can be calculated from the Poynting vector [5].

$$\underline{S}_{port\ i} = P + jQ = \int\limits_{port\ i} \underline{\mathbf{S}} \cdot \mathbf{n}\, d\Gamma_i$$

$$\underline{S}_{port\ i} = \frac{1}{2} \int\limits_{port\ i} (\mathbf{E} \times \mathbf{H}^*) \cdot \mathbf{n}\, d\Gamma_i \qquad (38)$$

The apparent power through port 4 is the sum of the reflected waves from port 2 and port 3. The lengths of the arms connected to port 1, port 2 and port 4 are $0.1m$. To maximize the signal strength on port 4, the length of the arm to port 3 has been altered to $0.1m + \lambda/4$, where λ is the wave length. The walls of the waveguide are modeled as perfect conductors. The problem was investigated at $10GHz$.

Both for the $\mathbf{A}, V$ and the $\mathbf{T}, \Phi$ formulations, the PML parameters were set to the following values: $a = b = e = 2$, $h = 27,43mm$, $r_{min} = r_{max} = 0.2m$, $\beta = 209.44$, $\rho_{ref} = 10^{-4}$ and $d = 3{*}10^{-3}$. To investigate the accuracy of the PML, different numbers n of PML layers have been used. The thickness h of one PML layer was calculated for the $\mathbf{A}, V$ formulation and for the $\mathbf{T}, \Phi$ formulation using (31) as follows:

$$h_{min} \geq \frac{-\ln \rho_{ref}}{k_n \left(\frac{1}{r_{max}} + \beta\right) 2 \cdot n \cdot e} = \frac{10.74E{-}3}{k_n \cdot n}[m]$$

$$h_{max} \leq \frac{-\ln d}{k_n \left(\frac{1}{r_{min}} + \beta\right) 2 \cdot e} = \frac{6.77E{-}3}{k_n}[m] \qquad (39)$$

Furthermore, the effect of a lossy linear material to the reflection coefficient has been investigated. The reflection coefficient r_T at port 4 is defined as:

$$r_T = 10 \cdot \log\left(\frac{|\underline{S}_{Port4}|}{|\underline{S}_{Port1}|}\right) \qquad (40)$$

Fig.3 shows the reflection coefficient against the thickness of one PML layer for different numbers n of the PML layers. Fig.3(a) shows the result for the $\mathbf{A}, V$ formulation and Fig.3(b) shows the result for the $\mathbf{T}, \Phi$ formulation. Proper values for the reflection coefficient are those lower than $-40\ dB$. As can be seen the best values for thickness h of one PML layer can be obtained from the lower bound

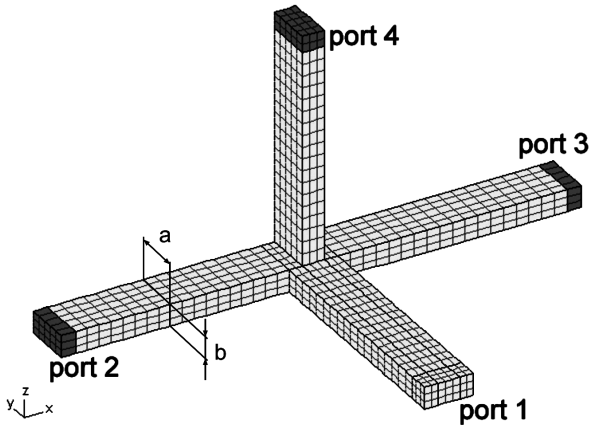

Figure 2. Waveguide hybrid junction, known as Magic-T. The PML layers are shown darker.

TABLE I: Reflection coefficient at interface lossy medium and PML

n	$\boldsymbol{\sigma}$ $[S/m]$	$r_T(\mathbf{A}, V)$	$r_T(\mathbf{T}, \Phi)$
3	0	2.34E-6	7.01E-6
	0.001	2.73E-6	4.15E-6
	0.01	2.98E-5	1.54E-5
	0.1	1.50E-7	3.53E-7
2	0	2.30E-5	2.23E-5
	0.001	2.85E-5	1.48E-5
	0.01	6.40E-5	3.81E-5
	0.1	5.74E-7	3.19E-7
1	0	1.34E-3	8.48E-5
	0.001	1.17E-3	6.30E-5
	0.01	4.97E-4	1.90E-5
	0.1	1.84E-8	2.34E-7

of (31). Furthermore, Fig.3 shows that the values for ρ_{ref} can be improved in dependence of the number n of PML layers for the $\mathbf{A}, V$ formulation

$$\rho_{\mathbf{A},V} = \begin{cases} 1 \cdot 10^{-4} & n \geq 4 \\ 2 \cdot 10^{-4} & n = 3 \\ 3 \cdot 10^{-3} & n = 2 \end{cases}, \qquad (41)$$

and for the $\mathbf{T}, \Phi$ formulation

$$\rho_{\mathbf{T},\Phi} = \begin{cases} 2 \cdot 10^{-4} & n \geq 3 \\ 5.5 \cdot 10^{-3} & n = 2 \\ 4.5 \cdot 10^{-3} & n = 1 \end{cases}. \qquad (42)$$

Table I shows the dependence of the reflection coefficient r_T on the losses in the medium. For this investigation the whole Magic-T has been filled with the lossy material. The best values for the reflection coefficient from Fig.3 have been chosen to evaluate the impact of the losses on the reflection coefficient of the anisotropic absorber. Losses lower than $0.001S/m$ do not change the reflection coefficient dramatically and losses higher than $0.1S/m$ damp too much for a proper wave propagation.

To demonstrate the difference between the $\mathbf{T}, \Phi$ formulation and the $\mathbf{A}, V$ formulation with one PML layer, Fig. 4 has been plotted. Fig. 4(a) shows the electric field in the Magic-T with the $\mathbf{T}, \Phi$ formulation. As can be seen,

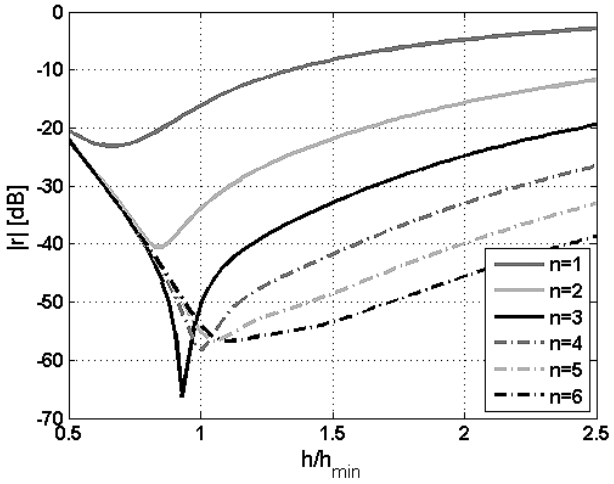

(a) $\mathbf{A}, V$ formulation

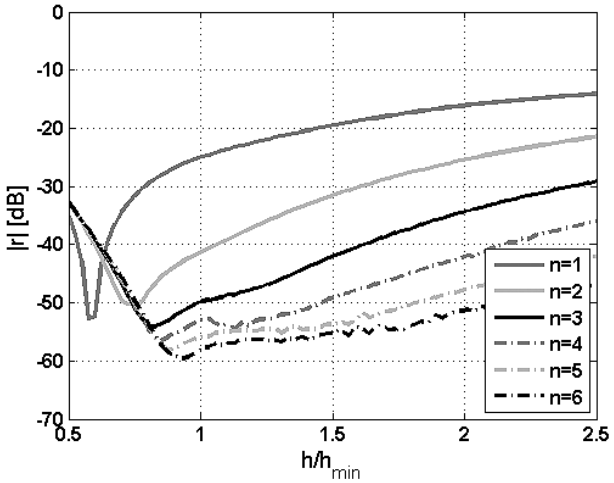

(b) $\mathbf{T}, \Phi$ formulation

Figure 3. Reflection coefficient against the thickness of the PML for different number of PML layers

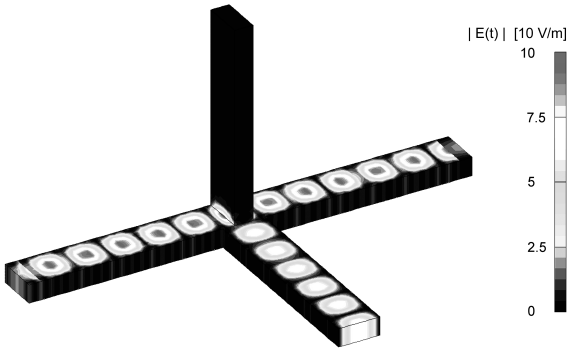

(a) $\mathbf{T}, \Phi$ formulation

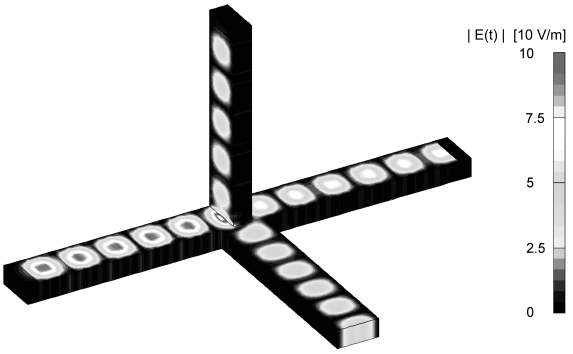

(b) $\mathbf{A}, V$ formulation

Figure 4. Electric field in the waveguide calculated with one PML layer

the PML layer works properly, there is no visible field at port 4. Figure 4(b) shows the electric field in the Magic-T with the $\mathbf{A}, V$ formulation. There is a visible electric field at port 4 showing that the reflection at port 2 and port 3 is too high. This example shows that it is adequate to use only one PML layer with the $\mathbf{T}, \Phi$ formulation. In addition, the reflection of the PML layers can be decreased if the thickness of the layers is tuned.

B. Dipole Antenna

For the second example, a $\lambda/2$-dipole antenna has been treated [6]. Making use of symmetry, one eighth of the arrangement was modeled only. The edge size of the cube was 2λ and its material constants were $\epsilon_r = 4$, $\mu_r = 1$ and $\sigma = 0.2\ mS/m$. An excitation frequency of $2.5\ GHz$ has been chosen. The antenna was modeled as a cylindrical wire with a diameter of $1\ mm$. The walls of the antenna were modeled as perfect electric conductors.

For the $\mathbf{T}, \Phi$ formulation one and two PML layers were used and for the $\mathbf{A}, V$ formulation three PML layers were applied. The PML parameters were set to the following values: $a = b = e = 2$, $r_{min} = 0.12m$, $r_{max} = 0.2m$, $\beta = 104.8$ and $d = 3 * 10^{-3}$. The thickness of one PML layer was calculated for the $\mathbf{A}, V$- and $\mathbf{T}, \Phi$ formulation with the lower bound of equation (31) using (41) and (42). Fig. 5 shows the finite element model of the $\lambda/2$-dipole antenna. The PML layer is plotted darker and the $\lambda/2$-dipole antenna is drawn black.

Fig 6 shows the radiation pattern [7] obtained from the simulation of the $\lambda/2$-dipole with the $\mathbf{A}, V$ formulation. The radiation pattern from the simulation is the same as the well known analytic radiation pattern of a $\lambda/2$-dipole.

The field plots for the electric field obtained from the $\mathbf{T}, \Phi$ formulation are shown in Figs 7(a) and 7(b) and the field obtained by the $\mathbf{A}, V$ formulation is plotted in Fig 7(c). The solutions for the electric field look quite the same for both formulations. The PML layers are plotted in light gray in all figures. The excitations for the $\mathbf{T}, \Phi$ formulation and for the $\mathbf{A}, V$ formulation have not been scaled equally. The deviation between the two solutions is very small indicating that the PML also works with free space wave propagation for a $\mathbf{T}, \Phi$ formulation.

V. CONCLUSION

It has been shown that it is possible to truncate any linear lossless material with PML layers, and if the material has small losses the PML works fine. It also has been shown that the reflectionless truncation of the problem boundaries using FEM also works with the $\mathbf{T}, \Phi$ formulation. Furthermore, for the $\mathbf{T}, \Phi$ formulation it is possible to use one PML layer only. The reflection at the PML layer is better

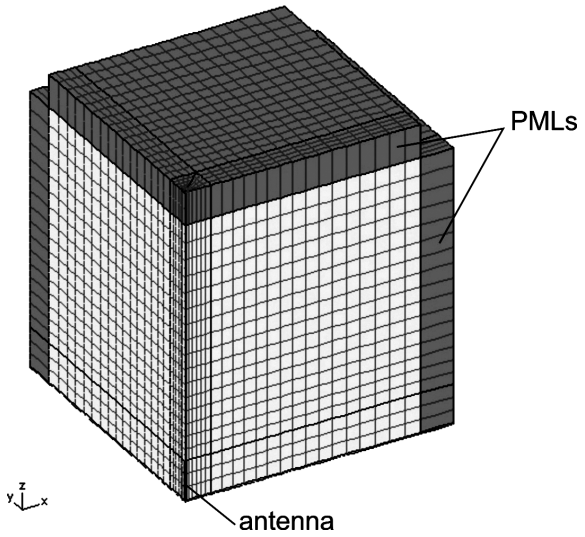

Figure 5. Finite element model of a $\lambda/2$ dipole antenna. PML layers are shown darker. $1/8$ of the structure modeled.

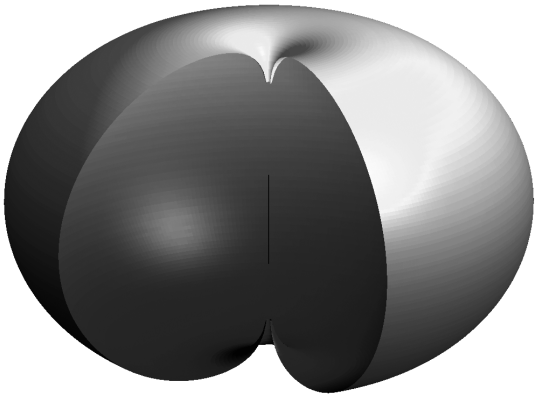

Figure 6: Radiation pattern for a $\lambda/2$-dipole antenna

at the lower bound of (31) for the complex PML constant. In addition the PML implementation can be improved by reducing the layer thickness h by varying ρ as shown in (41) and (42).

REFERENCES

[1] O. Bíró, "Edge element formulation of eddy current problems," *Computer methods in applied mechanics and engineering*, Volume 169, 1999, pp.391-405.

[2] Z.S. Sacks, D. M. Kingsland, R. Lee and J. F. Lee, "A perfectly matched anisotropic absorber for use as an absorbing boundary condition," *IEEE Transactions on Antennas and Propagation*, Volume 43, Issue 12, Dec. 1995 pp.1460 - 1463.

[3] I. Bárdi, O. Bíró, K. Preis, W. Renhart, "Parameter estimation for PMLs used with 3D finite element codes," *IEEE Transactions on Magnetics*,Volume 34, Issue 5, Part 1, Sept. 1998 pp.2755 - 2758.

[4] R.E. Collin, "Foundations for Microwave Engineering,"*McGraw - Hill International Editions*, Singapore 1992, 2nd Edition, pp.435 ff.

[5] K. Simonyi, "Theoretische Elektrotechnik," *Barth-Verlag*, Leipzig 1993, 10. Aufl., pp.65ff.

[6] R.C. Hansen, "Fundamental limitations in antennas," *Proceedings of the IEEE*, Volume 69, Issue 2, Feb. 1981 pp.170 - 182

[7] G.S. Smith, "An introduction to classical electromagnetic radiation," *Cambridge University Press*, 1997, 5th ed. , pp.218ff.

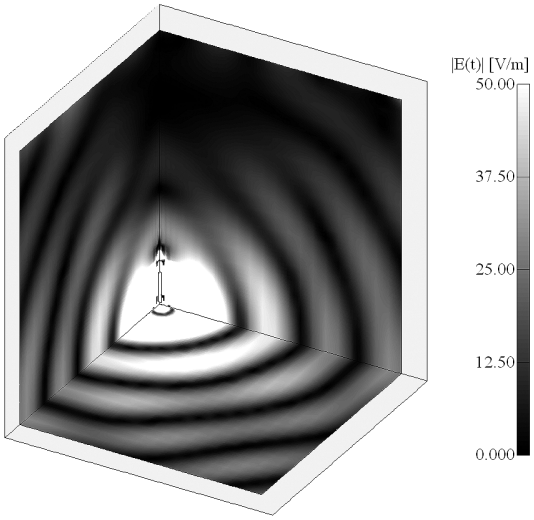

(a) One PML layer - $\mathbf{T}$, Φ formulation

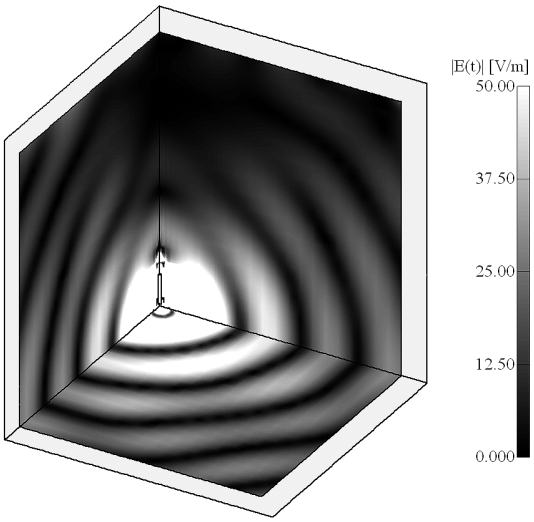

(b) Two PML layers - $\mathbf{T}$, Φ formulation

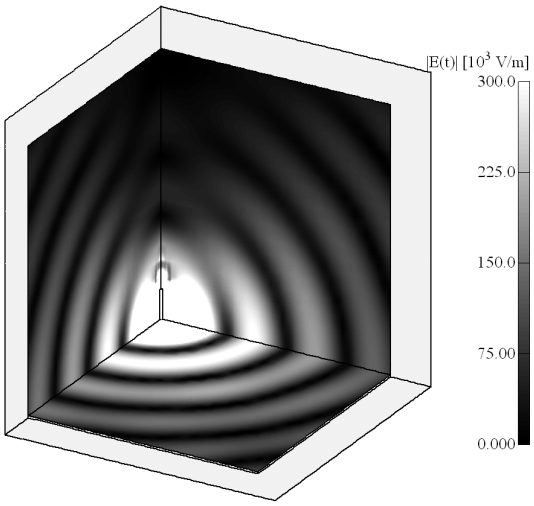

(c) Three PML layers - $\mathbf{A}$, V formulation

Figure 7. Field plot for the electric field for $\mathbf{T}$, Φ formulation and $\mathbf{A}$, V formulation with different numbers of PML layers.